

# CO<sub>2</sub> Decomposition Using Glow Discharge Plasmas

Jin-Yun Wang,\* Guan-Guang Xia,† Aimin Huang,\* Steven L. Suib,\*†‡<sup>1</sup> Yuji Hayashi,§  
and Hiroshige Matsumoto¶

\*U-60, Department of Chemistry, University of Connecticut, Storrs, Connecticut 06269-4060; †Institute of Materials Sciences, University of Connecticut, Storrs, Connecticut 06269; ‡Department of Chemical Engineering, University of Connecticut, Storrs, Connecticut 06269; §Fujitsu Laboratories, Ltd., 1015 Kamikodanaka, Nakahara, 211 Japan; and ¶Department of Chemistry, Nakasaki University, Bunkyo-machi 1-14, Nakasaki, 852 Japan

Received December 4, 1998; accepted March 15, 1999

Carbon dioxide decomposition has been studied using ac glow discharge plasmas at atmospheric pressure. A tubular reactor with a metal rod inside a quartz tube was wrapped with aluminum foil. The reaction mixture was analyzed by using a mass spectrometer. No coke deposits or other side reactions were observed. A variety of parameters, such as different metals, CO<sub>2</sub> concentrations, flow rate of the CO<sub>2</sub> containing gas, frequency, and power were investigated. The effects of these parameters on CO<sub>2</sub> conversion, reaction rates, and energy efficiency were examined. The initial excitation voltage to produce the plasma is independent of the metal identity on the surface of the rod and the flow rate of CO<sub>2</sub> containing gas, but dependent on the CO<sub>2</sub> concentration and ac frequency used. The maximum energy efficiency was obtained with relatively high CO<sub>2</sub> concentration, high flow rate of CO<sub>2</sub> containing gas, high frequency, as well as low input voltage at the expense of conversion.

© 1999 Academic Press

## I. INTRODUCTION

Carbon dioxide, the complete oxidation product of fossil fuel and organic compounds, is the most important greenhouse gas. More than half of the enhanced greenhouse effect is caused by the increase of carbon dioxide concentration in air (1–4). Since utilization of fossil fuels will continue to be a major energy source, CO<sub>2</sub> emission to the air will increase, and the greenhouse effect is expected to be more severe in the near future (5). The remediation of CO<sub>2</sub> has received increasing attention (6–9).

Hydrogenation of CO<sub>2</sub> and CO<sub>2</sub> reforming of methane have been the two major chemical reactions carried out by conventional catalytic methods. The high cost of H<sub>2</sub> and the unfavorable reverse water–gas shift reaction limited practical applications of hydrogenation of CO<sub>2</sub> (10, 11). Even though a great deal of research has also been done in CO<sub>2</sub> reforming of methane (8, 12, 13), the reaction requires high temperatures or high energy input due to the inertness of CO<sub>2</sub>.

Chemical absorption by a basic liquid, as well as absorption of CO<sub>2</sub> by zeolite-packed bed filters or CO<sub>2</sub> separation by polymer membranes (14), have been proposed for fossil power plants. These proposals increase construction cost of power plants by 70%, and decrease overall power plant efficiency from 42 to 34% (14).

Researchers have long been exploring different new ways, such as plasma processes, for reduction of CO<sub>2</sub>. CO<sub>2</sub> breakdown into CO or coke (15–17) and additional gaseous component effects (Ar, N<sub>2</sub>, and H<sub>2</sub>) (18) have been intensively investigated. Corona-induced plasma reduction of CO<sub>2</sub> has been a very active research area using either Corona torches (19) or ferroelectric packed bed reactors (14). The possibility of efficient processes for CO<sub>2</sub> reduction was demonstrated.

We have extended our interests from low pressure microwave plasmas for oligomerization of methane (20, 21) to atmospheric ac glow discharge plasmas using different type of reactors (22, 23). The decomposition of CO<sub>2</sub> using a fan-type reactor has been studied in our laboratories, and very high conversion was achieved (23). In this work, we present CO<sub>2</sub> dissociation using glow discharge plasmas with tubular reactors. A tubular reactor consists of a quartz tube wrapped with aluminum foil which served as an anode and a stainless steel rod coated with different metals as cathodes in the center of the quartz tube.

## II. EXPERIMENTAL

### 2.1. Reactor

The decomposition reactions of CO<sub>2</sub> were conducted in a tubular reactor (24, 25). The reactor consisted of a 20-cm quartz tube with outside diameter (o.d.) of 12 mm and inside diameter (i.d.) of 10 mm. A metal rod (30 cm) with diameter of 8 mm was put inside the quartz tube. Two sets of special T-type three-way valves at both ends of the quartz tube were used. One valve served as an inlet and the other served as an outlet for the gas flow. Two sets of bearings and nuts were used to keep the metal rod in the center position and

<sup>1</sup> To whom correspondence should be addressed.

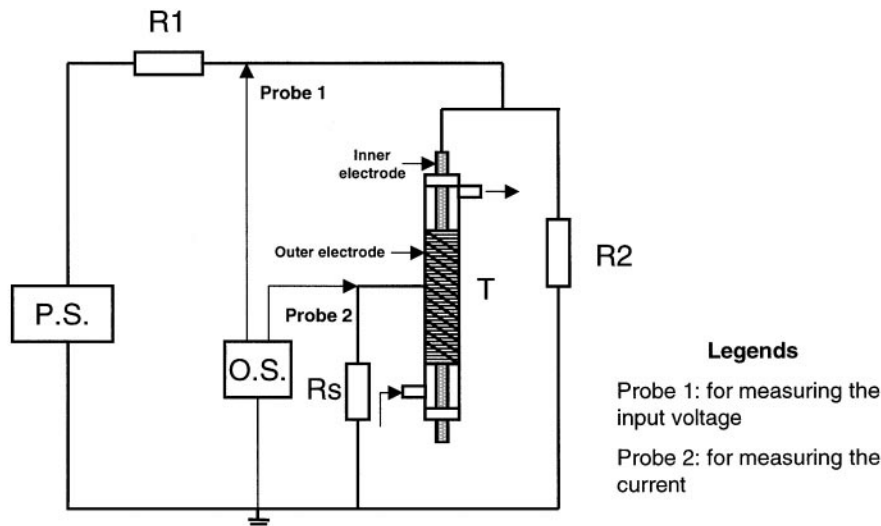


FIG. 1. Circuit diagram of the reaction system. P.S., power supply; O.S., oscilloscope; T, tubular reactor; R<sub>1</sub>, resistor 1; R<sub>2</sub>, resistor 2; R<sub>s</sub>, standard resistor.

to seal the openings of the metal rod and the valves. A piece of aluminum foil with a width of 10 cm was wrapped around the quartz tube and copper wire was used to fix the foil. A variety of metals (Au, Pd, Pt, and Rh) were coated using electroless plating on copper or stainless steel rods. The reactor configuration produces a gap of 1 mm between the metal rod and the inside of the quartz tube and 2 mm between the metal rod and the aluminum foil.

## 2.2. Experimental Setup

A schematic experimental setup is shown in Fig. 1. A Japan-Inter UHV-10 ac high voltage generator with fixed frequency of 8.1 kHz and a Trek high voltage amplifier and Wavetek function generator with changing frequency (1 to 6 kHz) were used to produce a potential across the gap. The changing current and voltage of the plasma reaction were monitored with a Yokogawa digital oscilloscope DL 1520 with a Tektronix 6015A high voltage probe when the UHV-10 ac high voltage generator was used. The current was measured with a 10 Ω standard resistor in series with the reactor during voltage drop. An input ac voltage of 1.0 to 7.0 kV with the UHV-10 high voltage generator or 2.5 to 14.4 kV with the Trek Wavetek function generator was employed across the gap. The CO<sub>2</sub> concentrations were varied from 1.0 to 10% balanced with He gas and the flow rates ranged from 10 to 60 mL/min.

The reaction mixture was analyzed using an MKS-UTI PPT quadrupole residual gas analyzer mass spectrometer (MS) with a variable high pressure sample manifold and a Faraday cup detector. CO<sub>2</sub> conversion was calculated based on the change in the signal of the  $m/e = 44$  peak. The signal is proportional to the partial pressure of CO<sub>2</sub> in the gas mixture in the range of concentration studied. CO and O<sub>2</sub> prod-

ucts were calculated based on the increase of the  $m/e = 28$  and  $m/e = 32$  signals, respectively. All the data collected were at steady state, which could be reached within a few minutes depending on the flow rate of the reaction mixture.

## III. RESULTS

### 3.1. Variation of Plasma Generation with CO<sub>2</sub> Concentration and Input Voltage

The minimum input voltage, or initial excitation voltage, required to generate plasmas (see Fig. 2) was found to be dependent on the CO<sub>2</sub> concentration, but independent of the coated metals on the rod and flow rates of the gas stream for the reactor setup using the UHV-10 high voltage generator. For pure He gas, the initial excited voltage is ca 1.0 kV. The initial excited voltage is higher in the presence of CO<sub>2</sub>, and higher CO<sub>2</sub> concentrations require higher input voltages to initiate the plasma. The initial excitation voltage for pure CO<sub>2</sub> is ca. 6.8 kV.

### 3.2. Metal Effects on the CO<sub>2</sub> Conversion

Different metal rods were used to study the plasma reactions. Figure 3 shows the CO<sub>2</sub> conversion vs input voltage for different metals with 4.0% CO<sub>2</sub> in He gas at a flow rate of 20 mL/min. The general trend for all metals was that the conversion of CO<sub>2</sub> increased with increasing input voltage. The slope of the CO<sub>2</sub> conversion was larger at low input voltage and leveled off at high input voltage. The CO<sub>2</sub> conversion using a Au rod started to decrease at input voltages >5 kV. The order of activity was Cu > Au > Rh > Fe ≈ Pt ≈ Pd.

The quartz tube was found to be hot (ca. 60°C) after application of a high voltage (≥5 kV). If an external fan was

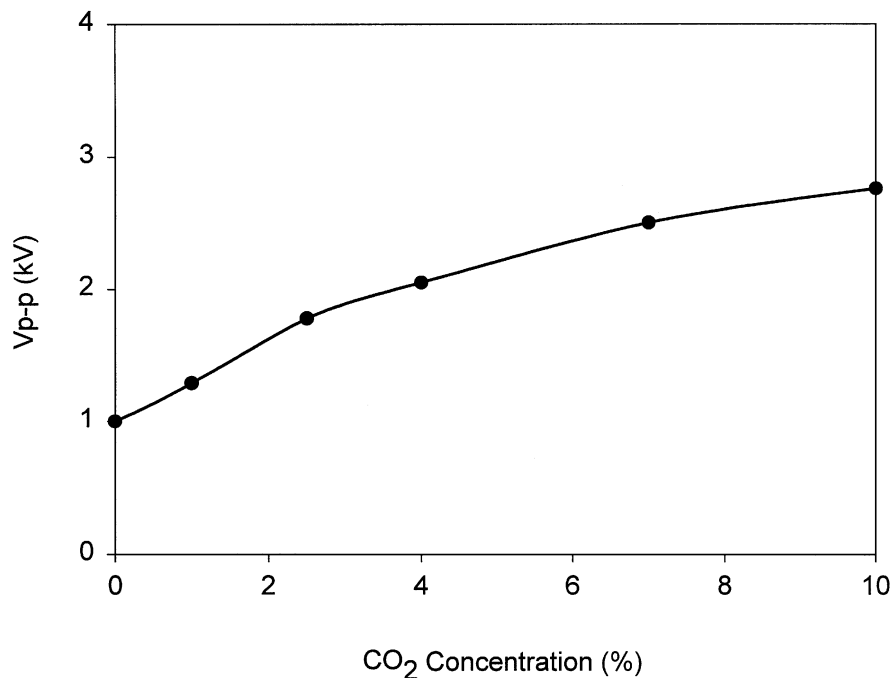


FIG. 2. Initial excitation voltage vs CO<sub>2</sub> concentration at frequency of 8.1 kHz.

used to cool the reactor, conversion of CO<sub>2</sub> for all metals gained 0.5–3% (when  $V_{p-p} \geq 5$  kV) compared to no cooling. No conversion drop was observed for Au up to 6 kV. Cu was chosen for the following studies because Cu is active

and shows less of a thermal effect. No external fan was used for further studies.

The energy efficiency of the reactor was defined as  $\Delta H/E_p \times 100$ , where  $\Delta H$  (257 kJ/mol) is the enthalpy of

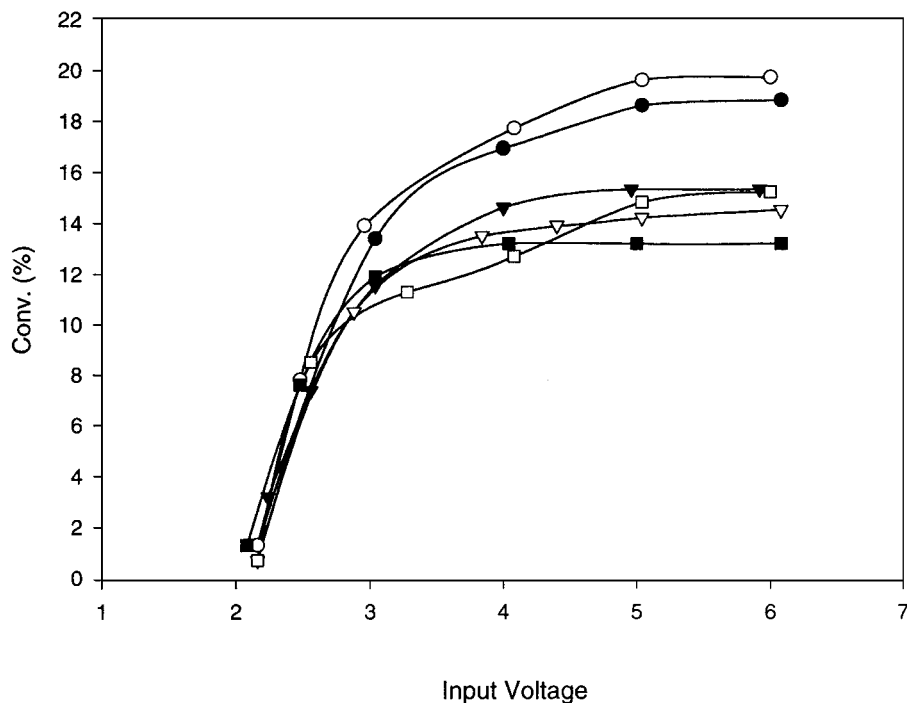


FIG. 3. CO<sub>2</sub> conversion change vs input voltage for different metal rods at flow rate of 20 mL/min. ●, Au; ○, Cu; ▼, Rh; ▽, Fe; ■, Pd; □, Pt.

TABLE 1

Plasma Variables as a Function of Input Voltage ( $V_{p-p}$ ) for Different Metal Coated Reactors (4.0% CO<sub>2</sub> in He, 20 mL/min)

Metal	Power (W)	Conv. %	Efficiency %
Input voltage: $V_{p-p} = 2.48$ kV			
Au	0.11	7.3	9.344
Cu	0.12	7.28	8.54
Fe	0.13	6.2	6.72
Pd	0.18	7.55	5.91
Pt	0.16	6.4	5.63
Rh	0.24	6.15	3.61
Input voltage: $V_{p-p} = 4.0$ kV			
Au	0.34	16.1	6.67
Cu	0.66	17.0	3.63
Fe	0.69	13.6	2.78
Pd	0.71	13.0	2.58
Pt	0.71	15.8	3.13
Rh	0.79	14.6	2.60
Input voltage: $V_{p-p} = 6.0$ kV			
Au	1.68	19.2	1.61
Cu	1.73	19.4	1.58
Fe	1.81	13.2	1.03
Pd	1.74	12.9	1.04
Pt	2.10	14.2	0.95
Rh	1.88	15.3	1.15

decomposition of CO<sub>2</sub> to CO and O<sub>2</sub> and  $E_p$  is the energy consumed to convert 1 mol of CO<sub>2</sub> in the plasma. The variation of energy efficiency had an order similar to that of the activity for the different metals studied at the same input voltages shown in Table 1. Even though conversion of CO<sub>2</sub> increased with increase of input voltage for all the metals, the energy efficiency decreased with increasing input voltage. The energy efficiency was 9.34% for Au at an input voltage of 2.48 kV and 1.61% at an input voltage of 6.0 kV.

### 3.3. Effects of CO<sub>2</sub> Concentration and Input Voltage

A variety of CO<sub>2</sub> concentrations (1.0–10.0%) at different flow rates were studied as a function of input voltage. Figure 4a shows results at a flow rate of 40 mL/min, which are typical for other flow rates. The conversion of CO<sub>2</sub> at all different concentrations increased as the input voltage increased in the range of input voltage studied. Higher conversion was obtained with lower CO<sub>2</sub> content of the feed gas, and lower conversion was obtained with higher CO<sub>2</sub> content of the feed gas at the same input voltage. At  $V_{p-p} = 7.0$  kV, the conversion of 1.0% CO<sub>2</sub> in He was 33% and that of 10% CO<sub>2</sub> in He was only 8%. Data in Fig. 4a also indicate that the minimum input voltage needed to generate the plasma (or initiate conversion of CO<sub>2</sub>) increases as the CO<sub>2</sub> concentration increases.

The relationship between the reaction rate and input voltage for the reaction mixture with different CO<sub>2</sub> concentrations is shown in Fig. 4b. Generally, the reaction rate in-

TABLE 2

Effects of CO<sub>2</sub> Concentration on CO<sub>2</sub> Plasma and Energy Efficiency

% CO <sub>2</sub> in He	Power (W)	Conv. %	Efficiency %
1.0	0.506	21.2	2.95
2.5	0.630	19.4	5.42
4.0	0.653	13.4	5.78
7.0	0.710	8.5	5.90
10.0	0.805	6.9	6.03

Note. Cu rod as an inner electrode; flow rate = 40 mL/min; input voltage = 4.0 kV.

creased as the input voltage increased, but the slopes of the rate increases were different. The mixture with low CO<sub>2</sub> content tended to increase slowly and leveled off at a relatively low input voltage. The mixture with high CO<sub>2</sub> content increased the reaction rate quickly and continued to increase even at high input voltages. However, the mixture with the highest reaction rate was 7.0% rather than 10.0%.

Table 2 shows the effects of variation of CO<sub>2</sub> concentration on CO<sub>2</sub> conversion with a flow rate of 40 mL/min and an input voltage of 4.0 kV. The CO<sub>2</sub> conversion decreased from 21.2% for a CO<sub>2</sub> concentration of 1.0 to 6.9% for a CO<sub>2</sub> concentration of 10.0%. In contrast, the energy efficiency increased from 2.95% for a CO<sub>2</sub> concentration of 1.0 to 6.03% for a CO<sub>2</sub> concentration of 10.0%.

### 3.4. Effects of Input Voltage and Different Flow Rates

Different flow rates (20, 40, and 60 mL/min) were studied as a function of input voltage. The CO<sub>2</sub> reaction rates for a concentration of 4.0% are shown in Fig. 5, and the data are typical for other CO<sub>2</sub> concentrations. The general trend was that high conversion was obtained at low flow rates, and low conversion was obtained at high flow rates. In terms of reaction rates, low reaction rates were obtained at low flow rates, and high reaction rates were obtained at high flow rates at constant input voltage. The initial excitation voltages were ca. 2.0 kV, even though the flow rates were different.

Data in Table 3 show that trends of energy efficiency are opposite those of conversion as the flow rate varies. As the

TABLE 3

Effects of Flow Rate on CO<sub>2</sub> Plasma and Energy Efficiency

Flow rate (mL/min)	Power (W)	Conv. %	Efficiency %
20	0.66	17.0	3.62
40	0.653	13.4	5.78
60	0.663	11.0	7.01

Note. Cu rod as an inner electrode; 4.0% CO<sub>2</sub> in He; input voltage = 4.0 kV.

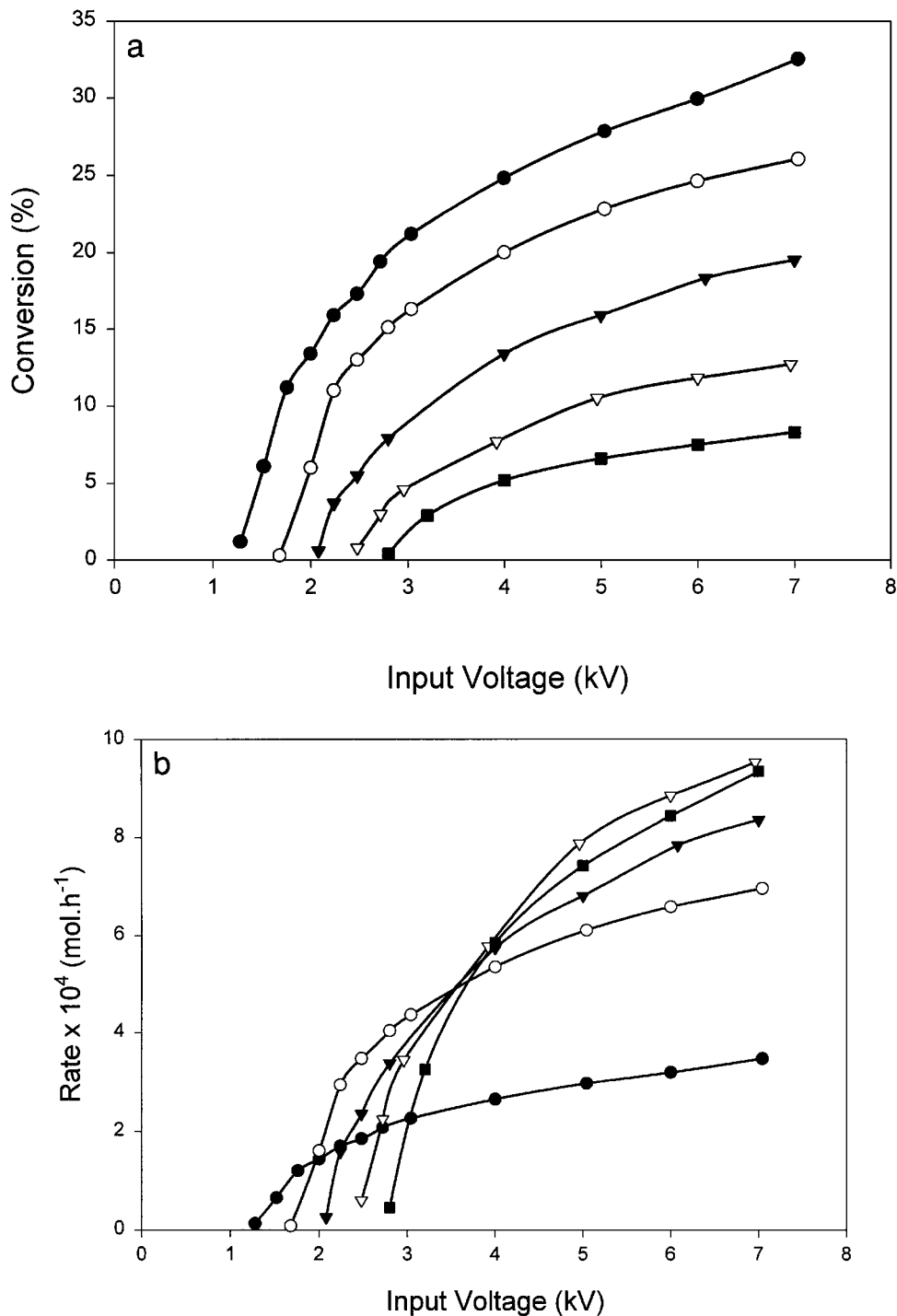


FIG. 4. (a) CO<sub>2</sub> conversion vs input voltage for different CO<sub>2</sub> content at flow rate of 40 mL/min. ●, 1.0%; ○, 2.5%; ▼, 4.0%; ▽, 7.0%; ■, 10.0%. (b) Reaction rate change vs input voltage for different CO<sub>2</sub> at flow rate of 40 mL/min. ●, 1.0%; ○, 2.5%; ▼, 4.0%; ▽, 7.0%; ■, 10.0%.

flow rate increased from 20 to 60 mL/min at an input voltage of 4.0 kV, the conversion of CO<sub>2</sub> decreased from 17.0% at a flow rate of 20 mL/min to 11.0% at flow rate of 60 mL/min, but the energy efficiency increased from 3.62% at a flow rate of 20 mL/min to 7.01% at a flow rate of 60 mL/min.

### 3.5. Variation of Plasma Parameters with Change of Frequency

The ac frequency was varied using a Trek high voltage amplifier and a Wavetek function generator. The results of

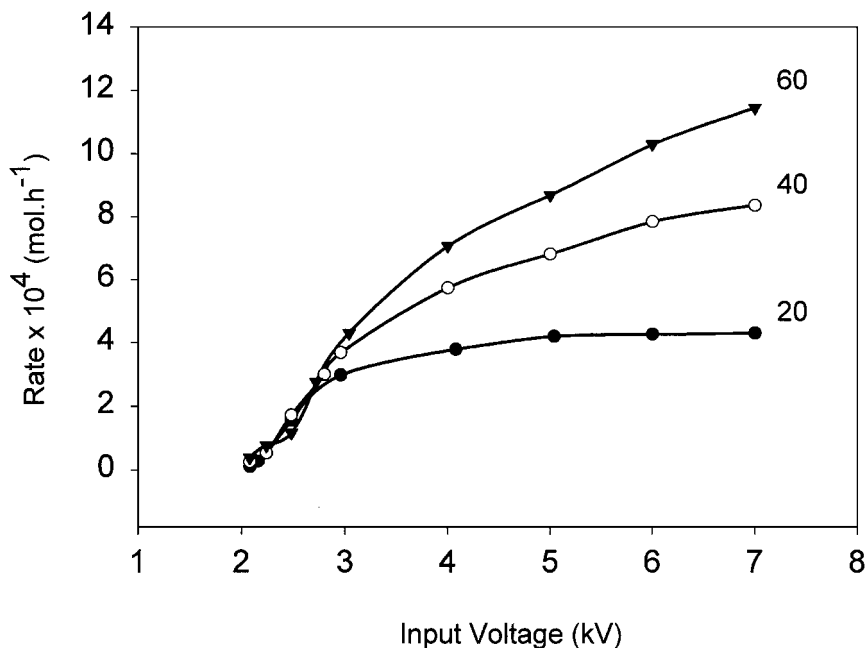


FIG. 5. Reaction rate change vs input voltage with different flow rate for CO<sub>2</sub> concentration of 4.0%. ●, 20 mL/min; ○, 40 mL/min; ▼, 60 mL/min.

conversion vs frequency at different input voltages for a 4.0% CO<sub>2</sub> mixture at a flow rate of 40 mL/min are shown in Fig. 6, which indicates that, at a fixed input voltage, conversion of CO<sub>2</sub> increases with increasing ac frequency and efficiency decreases with increasing frequency. Higher in-

put voltages produce higher CO<sub>2</sub> conversions at specific frequency. Data in Table 4 summarize the results of effects of frequency on CO<sub>2</sub> conversion and energy efficiency. As with the UHV-10 power supply, the energy efficiency of the reactor decreased with increasing CO<sub>2</sub> conversion at a fixed

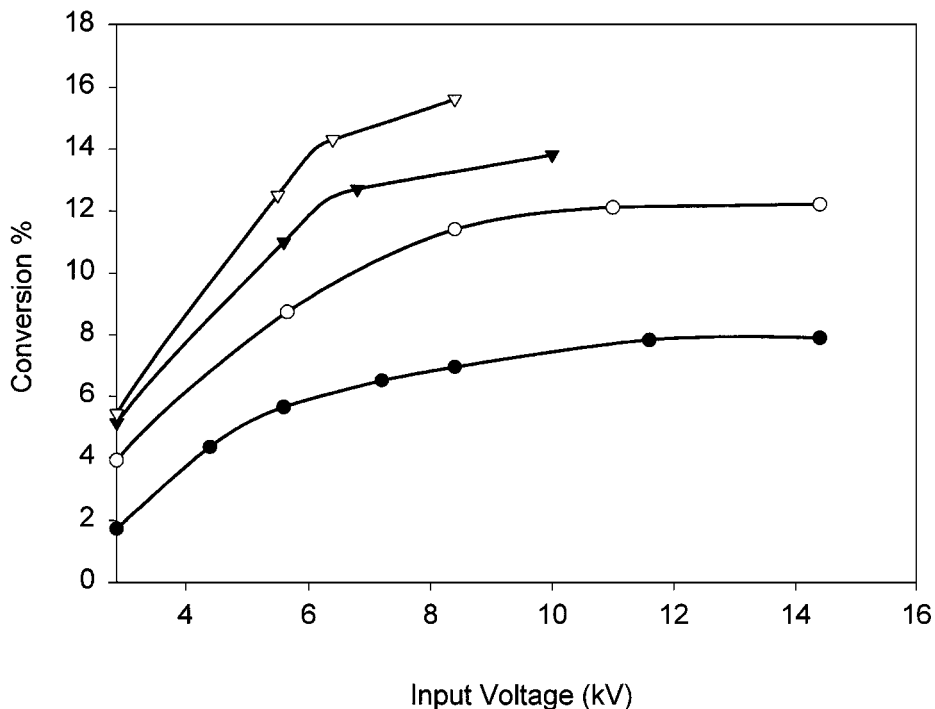


FIG. 6. CO<sub>2</sub> conversion vs input voltage for different frequency at flow rate of 40 mL/min with CO<sub>2</sub> concentration of 4.0%. ●, 1 kHz; ○, 2 kHz; ▼, 4 kHz; ▽, 5 kHz.

**TABLE 4**  
**Variation of Frequency on the Disassociation of CO<sub>2</sub>**

$V_{p-p}$ (kV)	$I$ (mA)	Power (W)	Conv. %	Efficiency %
Frequency: 1 kHz				
2.88	4.0	0.030	1.42	14.2
4.51	5.1	0.15	4.35	8.17
5.62	5.9	0.24	5.65	6.63
8.40	10.1	0.50	6.96	3.92
11.6	14.0	1.08	7.83	2.04
14.4	16.2	1.72	7.94	1.30
Frequency: 2.0 kHz				
2.64	3.8	0.024	1.31	15.4
2.88	4.9	0.10	3.92	11.0
5.60	12.1	0.51	8.75	4.83
8.40	17.8	1.20	11.8	2.77
11.0	25.6	2.08	12.1	1.64
14.4	32.1	3.66	12.2	0.94
Frequency: 4.0 kHz				
2.42	3.6	0.019	1.12	16.6
2.88	8.1	0.12	5.14	12.1
5.60	20.2	0.95	11.0	3.26
6.80	30.5	1.67	13.2	2.23
10.0	36.8	2.52	13.8	1.54

frequency. For example, as the input voltage increased from 2.64 to 14.4 kV at a frequency of 2 kHz, CO<sub>2</sub> conversion increased from 1.31 to 12.2%, but the energy efficiency of the reactor decreased from 15.4 to 0.94%.

## IV. DISCUSSION

### 4.1. Metal and Input Voltage Effects on Plasma Parameters

Figure 3 shows that initial generation or initial conversion of CO<sub>2</sub> occurs at an input voltage of ca. 2 kV for all the different metal rods studied. The initial excitation voltage is independent of the identity of the metal coatings on the rod. As the input voltage increases, the difference in CO<sub>2</sub> conversion becomes obvious. With input voltages  $\geq 3$  kV, the order of activity for different metals is the same as that of the metal's electrical conductivity, which is Cu > Au > Rh > Fe  $\approx$  Pt  $\approx$  Pd. The performance of metals at low input voltages showed no obvious differences, but significant differences were observed at high input voltage. This might be due to the properties of the metals and the quartz tube. The quartz tube is a dielectric material, and all the metals are good conductors.

The differences in electrical properties (such as conductivity) between different metals are rather insignificant compared to that of quartz. Charges will build up on the dielectric quartz as the input voltage increases, and the quartz tube behaves like a capacitor or a combination of a capacitor and a resistor in parallel with each other. Differences in metal character may emerge when the charges on the quartz tube become large enough. For this complicated sys-

tem, other factors, such as oxidation of surface metals on the rod, may be involved. Sputtering of Au was also observed as the Au thin layer gradually disappeared when the reaction was run for a period of 20 h. This implied that other physical or chemical properties might be important as well.

At high voltage, the resistance or impedance of the quartz reactor is decreased due to the formation of charged species, but the capacitance changes as input voltage and temperature increase which contribute to the low energy efficiency.

The trends in energy efficiency of different metals at different input voltages provide evidence that the reactor behaves like a combination of a capacitor and a resistor. The conversion of CO<sub>2</sub> increased sharply as the input voltage increased before the input voltage reached ca. 3 kV. The CO<sub>2</sub> conversion increased very slowly or even dropped for metals like Au and Cu at high input voltage. The decreasing energy efficiency at high input voltage observed for all metals may be due to energy consumption in order to overcome increases in resistance or impedance instead of use in chemical reactions. This is supported by observation of temperature increases of the reactor as high input voltages are imposed.

### 4.2. Effects of CO<sub>2</sub> Concentration and Input Voltage

Figure 4a indicates that higher input voltage is required to initiate CO<sub>2</sub> conversion as the CO<sub>2</sub> concentration increases. In other words, the initial excitation voltage increases with increasing CO<sub>2</sub> concentration. This is likely due to energy transfer from He to CO<sub>2</sub> (6). He is much more easily excited by the discharge than is CO<sub>2</sub>, as shown in Fig. 2. The excited or charged He particles tend to move from one electrode to another when a potential between the electrodes exists. Plasmas are produced and sustained when this movement is maintained.

The existence of plasmas can be monitored by the ac current which is evidence of charge migration (both electrons and ions). When charged He collides with uncharged He, such movement is due to transfer of energy and exchange of charge. The movement of charged particles will stop when charged He collides with CO<sub>2</sub> unless the energy is high enough to excite the CO<sub>2</sub> molecule. Since CO<sub>2</sub> is difficult to excite, CO<sub>2</sub> increases the resistance of the electrical gaseous layer. Higher CO<sub>2</sub> concentrations will provide more opportunities to annihilate the charged He particles of low energy. Therefore, high input voltage is required to produce and maintain the plasma reaction when high CO<sub>2</sub> content gas is used (27).

Even though the gas stream with higher CO<sub>2</sub> concentration produced lower CO<sub>2</sub> conversion at the same input voltage, the general trend was that the rate of CO<sub>2</sub> decomposition was higher for higher CO<sub>2</sub> content gas with the same input voltage or the same conversion. This means that high CO<sub>2</sub> concentration in the feed gas is preferred in order to better utilize the reactor. An optimal CO<sub>2</sub> concentration

seems to exist since the highest reaction rate obtained at high input voltage was for a CO<sub>2</sub> concentration of 7.0% instead of 10.0%. Data in Table 2 show that higher energy efficiency of the reactor was obtained with higher CO<sub>2</sub> concentration at the input voltage of 4.0 kV. The results indicate that high CO<sub>2</sub> content in the feed gas is desired in terms of space and energy efficiency when the input voltage is higher than 3.5 kV, which is indicated by Fig. 4b.

At low CO<sub>2</sub> content, energy transfer mainly occurs between He particles, and this plasma energy is not used to decompose CO<sub>2</sub>. This is why high CO<sub>2</sub> concentration is needed to obtain high energy and space efficiency. However, an optimal CO<sub>2</sub> content and input voltage may exist because high CO<sub>2</sub> content requires high input voltages to convert CO<sub>2</sub>, and high input voltages normally cause high energy consumption.

#### 4.3. Effects of Flow Rate

The initial excitation input voltage is independent of the flow rate of CO<sub>2</sub> because the conductivity of the gaseous layer does not change. The conductivity of the gaseous layer does not change as long as the composition of the mixture is constant. Higher energy efficiency was obtained at a flow rate of 60 rather than 20 or 40 mL/min. Conversion of CO<sub>2</sub> is lower at a higher flow rate, and lower CO and O<sub>2</sub> concentrations as well as the shorter residence times make the reverse reaction less probable. The high flow rate removes large amounts of heat from the reactor. High flow rates are preferred in terms of reactor efficiency and reaction rate, as implied by data of Fig. 5 and Table 3.

#### 4.4. Effects of Frequency on CO<sub>2</sub> Conversion and Plasma Parameters

Higher energy efficiency was obtained at lower frequency than that at higher frequency at similar input voltages. However, at similar conversion, higher energy efficiency was obtained at higher frequency rather than lower frequency. This might be due to low impedance at high frequency producing less heat and less consumption of energy than that seen under low frequency and high impedance conditions. The lowest energy needed to produce and sustain a plasma varied as the frequency changed, as shown in Table 4. This indicates that the initial excitation voltage is dependent on frequency at constant CO<sub>2</sub> concentration. In other words, in order to maintain plasma reactions at a certain CO<sub>2</sub> concentration, both input voltage and frequency need to be taken into account. The data at 8.1 kHz are consistent with this observation.

### V. CONCLUSIONS

The decomposition of carbon dioxide to produce CO and oxygen has been conducted using ac glow discharge plasmas. A tubular type reactor was used at atmospheric pres-

sure. A relative order of Cu > Au > Rh > Fe ≈ Pd ≈ Pt has been obtained for reactivity toward CO<sub>2</sub> decomposition. Even though CO<sub>2</sub> conversions were relatively lower than results using fan-type reactors (23), much higher energy efficiencies have been achieved. The initial excitation input voltage was found to be a function of CO<sub>2</sub> concentration and ac frequency, but independent of the identity of the metals coated on the surface of the inner electrode and the flow rate of the CO<sub>2</sub> containing gas. In order to obtain high reaction rates and high energy efficiencies, high frequency, a high flow rate of CO<sub>2</sub> containing gas, and a relatively high CO<sub>2</sub> concentration are preferred.

### ACKNOWLEDGMENTS

Dr. Stephanie L. Brock is acknowledged for helpful discussions. We also thank Fujitsu Ltd., Honda Research and Development, and Hokushin Co. for support of this research.

### REFERENCES

1. Edwards, J. H., *Catal. Today* **23**, 59 (1995).
2. Meehl, G. A., and Washington, W. M., *Nature* **382**, 56 (1996).
3. Sellers, P. J., Bounoua, L., Collatz, G. J., Randall, D. A., Dazlich, D. A., Los, S. O., Berry, J. A., Fung, I., Tucker, C. J., Field, C. B., and Jensen, T. G., *Science* **271**, 1402 (1996).
4. Knutson, T. R., Tuleya, R. E., and Kurihara, Y., *Science* **279**, 1018 (1998).
5. Tilley, J., *Energy Convers. Mgmt.* **34**, 711 (1993).
6. Ayers, W. M. (Ed.), "Catalytic activation of carbon dioxide," ACS Symposium Series 363. *American Chemical Society, Washington, DC, 1988.*
7. Dibby, D. M., Chang, C., Howe, R. F., and Yurchak, S., *Stud. Surf. Sci. Catal.* **36** (1988).
8. Mark, M. F., and Maier, W. F., *J. Catal.* **164**, 122 (1996).
9. Azar, C., and Rodhe, H., *Science* **276**, 1818 (1997).
10. Inui, T., *Catal. Today* **29**, 329 (1996).
11. Fisher, I. A., and Bell, A. T., *J. Catal.* **162**, 54 (1996).
12. Papp, H., Schuler, P., and Zhuang, Q., *Topics Catal.* **3**, 311 (1996).
13. Chang, J.-S., Park, S.-E., and Chon, H., *Appl. Catal. A* **145**, 111 (1996).
14. Jogan, K., Mizuno, A., Yamamoto, T., and Chang, J.-S., *IEEE Trans. Ind. Appl.* **29**, 876 (1993).
15. Moruzzi, J. I., and Phelps, A. V., *J. Chem. Phys.* **45**, 4617 (1996).
16. Cenian, A., Chernukho, A., Borodin, V., and Sliwinski, G., *Contrib. Plasma Phys.* **34**, 25 (1994).
17. Fridman, A. A., and Rusanov, V. D., *Pure Appl. Chem.* **66**, 1267 (1994).
18. Andreev, Y. P., Voronkov, Y. M., and Semiokhin, I. A., *Russ. J. Phys. Chem.* **49**, 394 (1975).
19. Maezono, I., and Chang, J.-S., *IEEE Trans. Ind. Appl.* **26**, 651 (1990).
20. Huang, J., and Suib, S. L., *J. Phys. Chem.* **97**, 9403 (1993).
21. Marun, C., Suib, S. L., Dery, M., Harrison, J. B., and Kablaoui, M. J., *J. Phys. Chem.* **100**, 17866 (1996).
22. Hayashi, Y., U.S. patent 08/139,907. Fujitsu Ltd., 1995.
23. Suib, S. L., Brock, S. L., Marquez, M., Luo, J., Hayashi, Y., Matsumoto, M., *J. Phys. Chem. B* **102**, 9661 (1998).
24. Tanaka, S., Uyama, H., and Matsumoto, O., *Plasma Chem. Plasma Proc.* **14**, 491 (1994).
25. Quintero, M. C., Rodero, A., Garcia, M. C., and Sola, A., *Appl. Spectrosc.* **51**, 778 (1997).
26. Lee, F. W., Collins, C. B., and Waller, R. A., *J. Chem. Phys.* **65**, 1605 (1976).
27. Blair, D. T. A., "Electrical Breakdown of Gases," pp. 533-653. Wiley, New York, 1978.